Draft version December 23, 2016
Preprint typeset using LaTeX style AASTeX6 v. 1.0

arXiv:1612.07464v1 [astro-ph.GA] 22 Dec 2016

FLUX AND POLARIZATION VARIABILITY OF OJ 287 DURING EARLY 2016 OUTBURST

Suvendu Rakshit [1,2], C.S. Stalin [1], S. Muneer [1], S. Neha [3, 4] and Vaidehi S. Paliya [1,5]

[1]Indian Institute of Astrophysics, Block II, Koramangala, Bangalore-560034, India
[2]suvenduat@gmail.com
[3]Aryabhatta Research Institute of Observational Sciences (ARIES), 263002, Nainital, India
[4]Pt. Ravishankar Shukla University, 492010, Raipur, India
[5]Department of Physics and Astronomy, Clemson University, Kinard Lab of Physics, Clemson, SC 29634-0978, USA

ABSTRACT

The gamma-ray blazar OJ 287 was in a high activity state during December 2015 - February 2016. Coinciding with this high brightness state, we observed this source for photometry on 40 nights in R-band and for polarimetry on 9 epochs in $UBVRI$ bands. During the period of our observations, the source brightness varied between 13.20 ± 0.04 to 14.98 ± 0.04 mag and the degree of polarization (P) fluctuated between $6.0 \pm 0.3\%$ and $28.3 \pm 0.8\%$ in R-band. Focusing on intra-night optical variability (INOV), we find a duty cycle of about 71% using χ^2-statistics, similar to that known for blazars. From INOV data, the shortest variability time scale is estimated to be 142 ± 38 min yielding a lower limit of the observed Doppler factor $\delta_0 = 1.17$, the magnetic field strength $B \leq 3.8$ G and the size of the emitting region $R_s < 2.28 \times 10^{14}$ cm. On inter-night timescales, a significant anti-correlation between R-band flux and P is found. The observed P at U-band is generally larger than that observed at longer wavelength bands suggesting a wavelength dependent polarization. Using V-band photometric and polarimetric data from Steward Observatory obtained during our monitoring period we find a varied correlation between P and V-band brightness. While an anticorrelation is seen between P and V-band mag at sometimes, no correlation is seen at other times, thereby, suggesting the presence of more than one short-lived shock components in the jet of OJ 287.

Keywords: BL Lacertae objects: individual: OJ 287 - polarization - galaxies: photometry

1. INTRODUCTION

OJ 287 is a well-known BL Lac object that shows featureless continuum spectrum. It has been extensively studied for optical flux variability (Blake 1970; Andrew et al. 1971; O'Dell et al. 1978). The long term optical light curve shows a well-defined 11.65 years of periodicity between large outbursts (Sillanpaa et al. 1988). Several models have been proposed to explain the periodicity in outburst such as the binary black hole model with the primary having an accretion disk (Sillanpaa et al. 1988, 1996), quasi-periodic oscillations in an accretion disc (Igumenshchev & Abramowicz 1999), and a binary black hole without relativistic precession (Katz 1997; Villata et al. 1998; Valtaoja et al. 2000). Among them, a precessing binary black hole in which the secondary black hole affects the accretion disk of the primary is more favorable than others as it predicts more accurately the timing of the major outburst (Sundelius et al. 1997; Valtonen & Ciprini 2012). OJ 287 has also been studied for polarization variability (Shakhovskoi & Efimov 1977; Sillanpaa et al. 1991, 1992; Valtaoja et al. 2000; Pursimo et al. 2000; Efimov et al. 2002; Villforth et al. 2009). Sillanpaa et al. (1991), based on the observations carried over six nights, found anticorrelation between flux and polarization variations which they explained as a result of highly rotating plasma inside a relativistic jet. However, Villforth et al. (2009) did not find any clear correlation between flux and polarization. From long term (year time scale) photopolarimetric observations, Efimov et al. (2002) noticed rapid continuous rotation of the position angle of about 4.92 degrees/day in clockwise direction suggesting a helical magnetic field jet structure. OJ 287 is also known to show variability and flares at GeV γ-ray energy (Ciprini et al. 2009; Escande & Schinzel 2011; Neronov & Vovk 2011; Agudo et al. 2011).

OJ 287 was predicted to have a major outburst in 2015 by Valtonen et al. (2011). In line with the prediction, many episodes of flaring behavior were noted since December 2015. Shappee et al. (2015) and Valtonen et al. (2016) reported a strong optical flare on 05 December 2015, wherein they found an increase in brightness of about 1.5 mag. The WEBT/GASP project (Larionov et al. 2015) reported that the source reached maximum

brightness in the J-band on 04 December 2015. During the same period, enhanced brightness was also reported by the SMARTS monitoring program (MacPherson et al. 2015) and also independently by Valtonen et al. (2015). In the X-ray band too, Swift/XRT observations (Wierzcholska & Siejkowski 2015; Ciprini et al. 2015; Valtonen et al. 2016) found the source in a high brightness level on 05 December 2015. The source was again detected in a flaring activity on 05 February 2016 (Zola et al. 2016).

We have been monitoring OJ 287 repeatedly for photometric and polarimetric variations since January 2016 (Paliya et al. 2016; Muneer et al. 2016). Here, we present our new R-band photometric observations obtained during 40 nights from 07 January 2016 to 11 April 2016 including 21 nights of intra-night optical variability (INOV) as well as $UBVRI$ polarimetry including the ones already reported by us in Paliya et al. (2016) and Muneer et al. (2016), and R-band intra-night polarization variability (INPV) on 3 nights. The main motivation behind this monitoring is to understand (i) the INOV nature of the source in its recent flaring state and (ii) the relation between total flux and polarization characteristics of the source. The paper is organized as follows. In Section 2 we present our observations and analysis, the results of our monitoring are reported in Section 3, followed by the discussion in Section 4. We summarize our results in Section 5. We adopt a cosmology $H_0 = 70\,\mathrm{km\,s^{-1}\,Mpc^{-1}}$ and $q_0 = 0$.

2. OBSERVATION AND DATA REDUCTION

2.1. *Photometry*

Photometric observations in R-band were carried out with a 1k × 1k CCD attached to the 0.75-m telescope at the Vainu Bappu Observatory (VBO) in Kavalur, India. The CCD has a pixel size of 24 microns, image scale of 0.48″/pixel, gain of 1.01 e^- ADU^{-1} and readout noise of 11.51 e^-. Due to weather constraints, on some nights we were able to get only few points but on 21 nights we obtained more than 20 frames which allowed us to study INOV of the source. The source was suitably placed in the CCD so as to get at least three comparison stars given in Fiorucci & Tosti (1996). The log of the photometric observations is given in Table 1. The images were analyzed using standard procedures in IRAF[1]. To get the optimum aperture for aperture photometry we followed the procedure described in Stalin et al. (2004).

2.2. *Polarimetry*

Polarimetric observations were carried out on a total of 9 nights, of which on 6 nights single epoch multi-band $UBVRI$ observations were performed and on three nights continuous monitoring was done in R-band. For polarimetric observations, two telescopes were used, one the 104 cm telescope, located at VBO and the other the 104 cm Sampurnand telescope located at the Aryabhatta Research Institute for Observational Sciences (ARIES), Nainital. At the telescope in VBO, a three-band, double beam photo-polarimeter was used, the details of which can be found in Srinivasulu et al. (2015). We used diaphragm of 20″ diameter for the observations. In addition to the $UBVRI$ bands, we also obtained polarimetric measurements in the light integrated in the $V - I$ spectral region; we refer to this band as R'. At ARIES, the ARIES Imaging Polarimeter (AIMPOL, Medhi et al. 2007) was used. A detailed description of AIMPOL and the techniques of polarization measurements may be found in (Ramaprakash et al. 1998; Rautela et al. 2004; Neha et al. 2016). All polarimetric data are presented in Table 2.

3. RESULTS

3.1. *Intra-night optical variability (INOV)*

To study INOV, we restricted to only observations carried out for a minimum of about two hours so as to ensure the availability of a sufficient number of photometric points to characterize INOV. DLCs of the OJ 287 was generated relative to two comparison stars present on the same CCD frame as described in Section 2. We note that the chosen optimum aperture for photometry on each night is often close to the median FWHM and the host galaxy has negligible effects in our photometry (Cellone et al. 2000). Some DLCs are shown in Figure 1. In the star-star DLCs (with the comparison stars having similar brightness to OJ 287) at certain epochs, deviant points are noticed due to non-photometric sky conditions. Such data points are identified if they are greater than 2σ, where σ is the standard deviation of the star-star DLCs. The number of such deviant points that are removed amounts to maximum of two data points each in less than half a dozen of observing nights. To ascertain the variability nature of OJ 207 on any given night, we have employed three criteria outlined below.

One method is based on the parameter C given by Jang & Miller (1997). It is defined as the ratio of the standard deviation of the source-comparison star (σ_s) and the comparison stars (σ) DLCs and is given as $C = \sigma_s/\sigma$. As the DLCs of OJ 287 were generated relative to two comparison stars, we obtained two values of C. The source is considered variable only when both the values of $C \geq 2.576$ (see, Paliya et al. 2013).

As an alternative to the widely used C-statistics, de

[1] IRAF is by the Association of Universities for Research in Astronomy, Inc. under cooperative agreement with the National Science Foundation.

Diego (2010) proposed the F-statistics. It is defined as the ratio of the variance of source-comparison star (σ_s^2) and the comparison stars (σ^2) DLCs and is given by $F = \sigma_s^2/\sigma^2$. To find the variability on any given night using F value, we compared both the F values (relative to the two comparison stars) with the critical F value, F_ν^α, where α is the significance level and ν is the degrees of freedom ($\nu = N_p - 1$ where N_p is the number of data points in the DLC). Following Paliya et al. (2013), we used $\alpha = 0.01$, which corresponds to a probability $p \geq 99\%$. The source is considered to be variable only if both the F values are greater than F_ν^α.

We also used χ^2-statistics (Kesteven et al. 1976) to characterize INOV. According to this, if the χ^2 value of a DLC exceeds the critical value, $\chi^2_{\alpha,\nu}$, with significance $\alpha = 0.01$, then the source is considered variable. χ^2-statistics is defined by

$$\chi^2 = \sum_{i=1}^{n} \frac{(D_i - < D >)^2}{\epsilon_i^2} \quad (1)$$

Here ϵ_i is the error of the measurement D_i, and $< D >$ is defined as

$$< D >= \frac{\sum_{i=1}^{n} \epsilon_i^{-2} D_i}{\sum_{i=1}^{n} \epsilon_i^{-2}} \quad (2)$$

We calculated the amplitude of variability (Ψ, Romero et al. 1999) from the DLCs as $\Psi = 100\sqrt{(D_{\rm max} - D_{\rm min})^2 - 2\sigma^2}\,\%$. Here, $D_{\rm max}$ and $D_{\rm min}$ are the maximum and the minimum in the DLC of OJ 287 relative to the comparison stars and σ^2 is the variance of the star-star DLC. Thus, corresponding to the two DLCs of the source with respect to the two comparison stars, we have two values of Ψ on each night. The results of the C, F and χ^2-statistics and Ψ for all the 21 DLCs are given in Table 3.

We also estimated the duty cycle (DC) of INOV of OJ 287 using the definition of Romero et al. (1999),

$$DC = 100 \frac{\sum_{i=1}^{n} N_i (1/\Delta t_i)}{\sum_{i=1}^{n} (1/\Delta t_i)} \text{ per cent}, \quad (3)$$

where $\Delta t_i = \Delta t_{i,\rm obs}(1+z)^{-1}$ is the duration of the monitoring session of the source on the $i^{\rm th}$ night after cosmological redshift (z) correction. If INOV is detected then $N_i = 1$, otherwise $N_i = 0$. We find an INOV $DC = 30$ % when variability was characterized using C-statistics. However, using F-statistics the DC increased to 45%, and further increased to 71 % considering χ^2-statistics. This enhanced DC is similar to what is known for blazars (Stalin et al. 2004).

We calculated the minimum variability time scale in our INOV data as $\tau = dt/\ln(F_1/F_2)$ following the definition given by Burbidge et al. (1974). Here, dt is the time difference between any two flux measurements F_1 and F_2. From our observed DLCs we calculated all possible time differences τ_{ij} for all allowable pairs of observations for which $|F_i - F_j| > \sigma_{F_i} + \sigma_{F_j}$. From the ensemble of τ_{ij} values, the minimum time scale is obtained as $\tau_{\rm var} = \min[\tau_{i,j}]$. Here, i runs from 1 to $n-1$, and j runs from $i+1$ to n, where n is the total number of data points. The uncertainties in the $\tau_{i,j}$ values are determined by propagating the errors in the flux measurements (Bevington 1969). Using this method on all the DLCs where INOV is detected we find a minimum $\tau_{\rm var}$ of 142 ± 38 min in the observations done on 07 April 2016.

3.2. *Long-term optical variability (LTOV)*

The time span of our monitoring program is large enough to search for LTOV. The LTOV light curve of OJ 287 from 07 January 2016 to 11 April 2016 is shown in Figure 2. The magnitude of OJ 278 was calibrated using the three standard stars as mentioned in section 3.1. Figure 2 shows OJ 287 is variable on day like time scale. During our monitoring program a change of about 2 mag was found within a few days.

3.3. *Polarization variability*

Intra-night polarization variability (INPV) of OJ 287 has been studied earlier by Villforth et al. (2009) who found about 16 % polarization. On the nights of 05, 06 and 10 April 2016, we have sufficient data points in R-band to characterize the INPV of OJ 287. The polarization properties displayed by the source on those three nights are plotted in the 1st three panels of Figure 3. We also have in total 7 epochs of R-band polarization measurements between February and April 2016. These observations are shown in the last panel of Figure 3. When more than one measurements are available on any particular night, we have taken their average value to study Long-term polarization variability (LTPV). From this Figure, it is clear that the source has shown INPV as well as LTPV.

We also studied the correlation between different observed quantities and the results are shown in Figure 4. The solid lines in these Figures are the linear least-squares fit to the data. A correlation between brightness and P is found on 05 April 2016. Less INPV was observed on 06 April 2016 with P changing by only 1.5 % while PA changed by about 7 degrees. On 10 April 2016, the source becomes fainter by about 0.2 mag than its brightness on 06 April 2016, however, P increased by 7% and PA decreased by about 20 degrees.

On the LTPV, we find a clear anticorrelation between source brightness and P. However, PA is found to be correlated with brightness. We also find a negative correlation between PA and P. Similar results have been found by Sillanpaa et al. (1991). The statistics of the

correlation analysis between the photometric and polarimetric properties of OJ 287 are shown in Table 4.

To characterize INPV in our data we used the χ^2-statistics (see section 3.1). We considered the source as variable in polarization if χ^2 value exceeds the critical value $\chi^2_{\alpha,\nu}$ with significance $\alpha = 0.01$. The fractional variability (FV) index of the source is defined by

$$FV = \frac{A_{\rm max} - A_{\rm min}}{A_{\rm max} + A_{\rm min}}. \quad (4)$$

Here, $A_{\rm max}$ and $A_{\rm min}$ are the maximum and minimum amplitude of variations in both P and PA. The results of INPV are given in Table 5. The DC of INPV is found to be 81 %, which is similar to the DC of about 77 % found by Andruchow et al. (2005) for radio selected BL Lacs for which OJ 287 belongs to.

Figure 5 shows the long term variation of PA observed in the month of April 2016. Linear least squares fit to the data gives a rotation rate of 5.8 degree/day. This rate is close to the rate of 4.92 degree/day, found by Efimov et al. (2002). The observed Q and U parameters are plotted in Figure 5. The average values of Q and U are $< {\rm Q} >= -12.2 \pm 0.2$ % and $< {\rm U} >= -0.1 \pm 0.2$ % respectively. This deviates from the origin implying the presence of a stable polarized component (see, Jones et al. 1985).

3.4. *Wavelength dependent polarization (WDP)*

On few epochs, we have polarization observations in $UBVRI$ bands. The multi-band polarization variations are shown in Figure 6. During all the epochs except that on 12 February 2016, P in U-band is larger than the other bands and thus OJ 287 showed WDP. The variation of P as a function of wavelength for different nights is shown in Figure 6. From the Figure, it is clear that on some epochs, both P and PA decreases with wavelength, although the anticorrelation of P and wavelength is stronger than PA with wavelength.

4. DISCUSSION

OJ 287 has shown remarkable optical flux and polarization variations during its recent bright state in December 2015 − April 2016. We find the source to show large amplitude and high duty cycle of INOV. A large amplitude flare (0.12 mag) with a slow rise and fast declining pattern was found on 29 February 2016. Though the exact mechanisms for the cause of INOV are not known, the observations reported here can be used to put constraints on the physical characteristics of the source. From our INOV observations, we find the shortest time scale of variability, $\tau_{\rm var}$ of 142 ± 38 min on 07 April 2016 that sets an upper limit on the size of the emission region, $R_s < 19.5 \times 10^{14}(\delta/10)$ cm, where δ is the Doppler factor.

We estimated the observed Doppler factor, δ_o, based on relativistic beaming model (Marscher & Scott 1980; Aharonian et al. 2007; Xiang & Dai 2007). Following Bessell (1979), the observed monochromatic flux (f_R) is calculated from the apparent R-band magnitude (m_R) of OJ 287 (see Figure 2) as $f_R = 3.08 \times 10^{-23} 10^{-0.4 m_R}$ W m^{-2} Hz^{-1}. The observed source-frame monochromatic luminosity (L_{ν_s}) at the frequency ν_s (considering ν_s as the V-band frequency) is calculated from f_R using

$$L_{\nu_V} = 4\pi D_L f_R \left[\frac{\lambda_R}{\lambda_V(1+z)}\right]^{\alpha} (1+z)^{-1} \quad (5)$$

where the luminosity distance $D_L = (cz/H_0)^2(1+z/2)^2$, λ_R and λ_V are the effective central wavelengths of R and V band respectively, and α is the spectral index. We used $\alpha = 1.62$, which is the average spectral index found by Efimov et al. (2002). Though blazars show spectral variations, the value of α used here is similar to the value found for OJ 287 and other blazars from power law fits to broad band optical data (Williamson et al. 2014).

Following Elvis et al. (1994), we estimated the observed bolometric luminosity as $L_B = 13.2 \nu_V L_{\nu_V}$ where ν_V is the V-band frequency. Considering the fact that any strong outburst having energy $\Delta L = |L_i - L_j|$ must occur on timescale larger than $t_{\rm min} = \tau_{\rm var}/(1+z) << t_{\rm cross}$ (light crossing time of R_s), the inferred efficiency of accretion, η_o can be calculated as $\eta_o \geq 5 \times 10^{-43} \Delta L / t_{\rm min}$ (Fabian & Rees 1979). For our observed $\tau_{\rm var} = 142$ min, we find $t_{\rm min} = 108$ min, during which the bolometric luminosity has changed by $\Delta L = 4.33 \times 10^{45}$ erg s^{-1} corresponding to $\eta_o = 0.33$. In the case of disk accretion, a rapidly rotating black hole has an intrinsic value of accretion efficiency (η_i) less than about 0.3 (Frank et al. 1986). As our calculated value is greater than 0.1, the observed INOV is due to relativistic beaming.

The δ_o can be computed from the relationships of $\Delta L(o) = \delta^{3+\alpha} \Delta L(i)$ and $t_{\rm min}(o) = \delta^{-1} t_{\rm min}(i)$ (Frank et al. 1986; Zhang et al. 2002), and using $\eta_o \geq 5 \times 10^{-43} \frac{\Delta L(o)}{t_{\rm min}(o)}$ and $\eta_i \geq 5 \times 10^{-43} \frac{\Delta L(i)}{t_{\rm min}(i)}$ we find

$$\delta_o \geq \left(\frac{\eta_o}{\eta_i}\right)^{\frac{1}{4+\alpha}}, \quad (6)$$

where 'o' and 'i' refer to the observed and intrinsic values. Since the value of η_i can be between 0.007 (nuclear reaction) to 0.32 (maximum accretion), we used $\eta_i = 0.05$ (a geometric mean value) in the above equation and found $\delta_o \geq 1.17$. Using this δ_o and observed $\tau_{\rm var}$ of 142 min, we found $R_s < 2.28 \times 10^{14}$ cm.

Considering that the variable emission seen in OJ 287 is due to synchrotron processes, and requiring that $\tau_{\rm var}$ to be shorter than the synchrotron lifetime of the rel-

ativistic electrons in the observer frame (Hagen-Thorn et al. 2008), the magnetic field (B) can be estimated as

$$t_{\rm syn} \propto 4.75 \times 10^2 \left(\frac{1+z}{\delta \nu_{\rm GHz} B^3} \right)^{1/2} \text{ days} \qquad (7)$$

Using the observed $\tau_{\rm var}$ and δ_o, we find $B \leq 3.8$ G. However, using $\delta = 10$ (Baliyan et al. 1996; Neronov & Vovk 2011; Marscher & Jorstad 2011), we find $R_s < 19.5 \times 10^{14}$ cm and $B \sim 1.8$ G. A Doppler factor of 17 has been reported by Aller et al. (2014) based on fits to monitoring observations of OJ 287 in the radio band. Using $\delta = 17$ we obtain $B \sim 1.5$ G, which is close to the value of 0.93 G found in the OJ 287 by Baliyan et al. (1996).

Analysis of the long term variation of PA based on our limited polarimetric observations give a rotation rate of 5.8 degrees/day, similar to the value of 4.92 degree/day found by Efimov et al. (2002). This is also in general agreement with the recent results obtained from dedicated optical polarimetric monitoring of blazars, which indicates that the rotation of the plane of optical polarization is a characteristics property of blazars (Blinov et al. 2016). The same set of polarimetric observations also find differences in the polarization properties of different sub-classes of blazars (Angelakis et al. 2016). In our polarimetric observations, shown in Figure 6, for most of the epochs we find P to decrease with wavelength. This is similar to that noted by Takalo et al. (1994), however, inconsistent with that observed by Tommasi et al. (2001). The observed WDP can be explained in terms of a two-component model identified with the jet that gives rise to the constant polarized component and the shock that gives rise to the more polarized component (Valtaoja et al. 1991). The presence of this stable polarized component is also evident in the position of the average Q and U values that deviate from zero in the Q vs U plane as seen in Figure 5.

If the accretion disk/host galaxy contributes significantly to the optical emission (in addition to the synchrotron jet emission) of OJ 287, one would have expected higher polarization at longer wavelengths (Malkan & Sargent 1982; Smith et al. 1986). This is not observed in any of our data except that obtained on 12 February 2016 during which epoch the source was in an intermediate brightness state. Also, in the broadband SED of OJ 287, emission from the accretion disk is not prominent (Massaro et al. 2003). Moreover, OJ 287 is a highly core dominated object[2] and thus, the contribution of accretion disk to the optical emission of OJ 287 is insignificant. Alternatively, in the binary black hole model of OJ 287, thermal flares are expected when the secondary black hole crosses the accretion disk of the primary black hole. Observations do indicate that such outbursts are not accompanied by increased optical polarization. However, secondary outbursts after the major one do show a correlated behavior in polarization as well, which could be due to the jet of the secondary black hole getting activated. Our polarization observations reported here are during February - April 2016, much later than the thermal outburst of December 2015 (Valtonen et al. 2016). This along with other observational evidences outlined above indicate that the polarization emission during our observations of OJ 287 is mainly due to synchrotron processes happening in the jet of the source.

The LTPV observations show a clear anticorrelation between P and optical brightness as well as between PA and P. These results agree with the polarization monitoring of OJ 287 by Sillanpaa et al. (1991). However, D'arcangelo et al. (2009) noticed a positive correlation between polarization and brightness which is contrary to what we have found. To check for the robustness of our results we looked for the availability of photometric and polarimetric data during the period of our observation. From the *Fermi* monitoring program of Steward Observatory (Smith et al. 2009) supporting the *Fermi* mission all-sky survey, we collected 48 epochs of polarimetric and 34 epochs of V-band photometric data between the period 12 January 2016 and 15 April 2016. The data set along with our observations are shown in Figure 7. The data set is divided into four segments based on the seasonal gaps (as shown by dotted lines) for detailed correlation analysis between flux and polarization variations.

In Figure 8, we show the observed relation between flux and polarization behavior of the source for the first three segments. The correlation between these quantities in segment 4 is shown in Figure 4 as the Steward observations have only two epochs of data in this segment. From Figures 8 and 4 it is evident that the brightness of the source positively correlates with polarization during segment 1 (January 2016), correlates negatively during segment 2 (February 2016) and segment 4 (April 2016) and not show any trend during segment 3 (March 2016). The PA positively correlates with P in segments 1 and 2, however, correlates negatively in segment 4 and no correlation in segment 3. The results of the correlation analysis are given in Table 6.

In the shock-in-jet model of blazar variability, a positive correlation between flux and polarization variations is expected (Marscher & Gear 1985) which could be due to the magnetic field getting aligned because of the shock. Alternatively, if the flux variability is due to the emergence of a new blob of plasma (identified as a VLBI

[2] The ratio of core to extended emission is >995 (Antonucci & Ulvestad 1985).

scale knot) which has either a chaotic magnetic field or a magnetic field that is misaligned with the large scale field, an anticorrelation between flux and polarization variations can be expected (Hagen-Thorn et al. 2002; Homan et al. 2002). The observed correlation and anticorrelation between total flux and polarized flux can also be explained by changes in the trajectories of the shocks propagating down the relativistic jets as postulated in the "swinging jets" model of Gopal-Krishna & Wiita (1992). From the observations of OJ 287 reported here we find varied behavior between flux and polarization variations, which could happen because of the presence of more than one emission region in the jet of OJ 287 (Marscher et al. 2008) or due to the interaction between the jet and accretion disk (Valtonen et al. 2008, 2016). Near simultaneous flux and polarization observations of blazars are very limited and observations on a large sample of blazars are needed, which will give important leads to our understanding on the emission processes in blazars.

5. CONCLUSIONS

We have carried out photometric (40 nights) and polarimetric (9 epochs) observations of OJ 287 coinciding with its high brightness state during December 2015 − February 2016. The key findings are summarized below:

1. From 21 nights of INOV observations we found the source to show INOV on few nights. Using C-statistics we found the DC of INOV as 30 %, which increases to 45% and 71 % on using the F-statistics and χ^2-statistics respectively. On nights when INOV is observed, Ψ is larger than 3%. The observed large amplitude ($> 3\%$) and high DC of INOV are similar to that known for blazars.

2. We find the shortest flux variability time scale of 142 ± 38 min on April 07, 2016. Using this we put constraints on the size of the emitting region and magnetic field strength as 2.28×10^{14} (19.5×10^{14}) cm and 3.8 (1.8) G using $\delta = 1.17$ (10) respectively.

3. Considering LTOV, we find that OJ 287 has varied by about 2 mag during the period of our observations. During this period, it showed a maximum and minimum brightness of 13.20 ± 0.04 mag and 14.98 ± 0.04 mag respectively. A change of ∼1 mag was noticed in March within 10 days.

4. From polarimetric observations, we find OJ 287 showed both INPV and LTPV. Considering the polarization variations during February to April 2016, minimum and maximum P of 6 ± 0.3 % and 28.3 ± 0.8 % in R-band was observed. During the same period PA varied between 60.6 ± 0.8 degrees and 130.6 ± 1.3 degrees respectively.

5. In U v/s Q plane, the average Q and U deviate from zero, indicating the presence of two optically thin synchrotron emission components contributing to the polarized emission from OJ 287 jet.

6. The P in different wavebands are correlated, with the polarization at shorter wavelengths generally larger than at longer wavelengths, thus showing a wavelength dependent polarization behavior. This demands that the observed polarization is due to synchrotron process happening in the jet of the source.

7. During most of the observing period an anticorrelation is observed between flux and polarization variations. A wide variety of correlations are also noticed between PA and P as well as between PA and brightness. Such a variety of relations observed between flux and polarization variations might be because of the presence of more than one emission components in the jet of OJ 287.

We are grateful for the comments and suggestions by the anonymous referee, which helped to improve the manuscript. It is our pleasure to thank Professor A. V. Raveendran and Mr. G. Srinivasulu for their valuable suggestions and timely help for the efficient operation of the photo-polarimeter. We also thank K. Sagayanathan, A. K. Venkataramana, R. Baskar, S. Surendharnath, A. Muniyandi, A. Ramachandran, M. Muniraj and the personnel of the technical divisions for their support to carry out the observations presented in this paper. Data from the Steward Observatory spectropolarimetric monitoring project were used. This program is supported by Fermi Guest Investigator grants NNX08AW56G, NNX09AU10G, NNX12AO93G, and NNX15AU81G.

REFERENCES

Agudo, I., Jorstad, S. G., Marscher, A. P., et al. 2011, ApJL, 726, L13

Aharonian, F., Akhperjanian, A. G., Bazer-Bachi, A. R., et al. 2007, ApJL, 664, L71

Aller, M. F., Hughes, P. A., Aller, H. D., Latimer, G. E., & Hovatta, T. 2014, ApJ, 791, 53

Andrew, B. H., Harvey, G. A., & Medd, W. J. 1971, Astrophys. Lett., 9, 151

Andruchow, I., Romero, G. E., & Cellone, S. A. 2005, A&A, 442, 97
Angelakis, E., Hovatta, T., Blinov, D., et al. 2016, MNRAS, 463, 3365
Antonucci, R. R. J., & Ulvestad, J. S. 1985, ApJ, 294, 158
Baliyan, K. S., Joshi, U. C., & Deshpande, M. R. 1996, Ap&SS, 240, 195
Bessell, M. S. 1979, PASP, 91, 589
Bevington, P. R. 1969, Data reduction and error analysis for the physical sciences
Blake, G. M. 1970, Astrophys. Lett., 6, 201
Blinov, D., Pavlidou, V., Papadakis, I., et al. 2016, MNRAS, 462, 1775
Burbidge, G. R., Jones, T. W., & Odell, S. L. 1974, ApJ, 193, 43
Cellone, S. A., Romero, G. E., & Combi, J. A. 2000, AJ, 119, 1534
Ciprini, S., Gasparrini, D., Reyes, L. C., et al. 2009, The Astronomer's Telegram, 2256
Ciprini, S., Perri, M., Verrecchia, F., & Valtonen, M. 2015, The Astronomer's Telegram, 8401
D'arcangelo, F. D., Marscher, A. P., Jorstad, S. G., et al. 2009, ApJ, 697, 985
de Diego, J. A. 2010, AJ, 139, 1269
Efimov, Y. S., Shakhovskoy, N. M., Takalo, L. O., & Sillanpää, A. 2002, A&A, 381, 408
Elvis, M., Wilkes, B. J., McDowell, J. C., et al. 1994, ApJS, 95, 1
Escande, L., & Schinzel, F. K. 2011, The Astronomer's Telegram, 3680
Fabian, A. C., & Rees, M. J. 1979, in X-ray Astronomy, ed. W. A. Baity & L. E. Peterson, 381–398
Fiorucci, M., & Tosti, G. 1996, A&AS, 116, 403
Frank, J., King, A. R., & Raine, D. J. 1986, S&T, 71, 579
Gopal-Krishna, & Wiita, P. J. 1992, A&A, 259, 109
Hagen-Thorn, V. A., Larionov, V. M., Jorstad, S. G., et al. 2008, ApJ, 672, 40
Hagen-Thorn, V. A., Larionova, E. G., Jorstad, S. G., Björnsson, C.-I., & Larionov, V. M. 2002, A&A, 385, 55
Homan, D. C., Ojha, R., Wardle, J. F. C., et al. 2002, ApJ, 568, 99
Igumenshchev, I. V., & Abramowicz, M. A. 1999, MNRAS, 303, 309
Jang, M., & Miller, H. R. 1997, AJ, 114, 565
Jones, T. W., Rudnick, L., Aller, H. D., et al. 1985, ApJ, 290, 627
Katz, J. I. 1997, ApJ, 478, 527
Kesteven, M. J. L., Bridle, A. H., & Brandie, G. W. 1976, AJ, 81, 919
Larionov, V. M., Arkharov, A. A., Efimova, N. V., Klimanov, S. A., & Di Paola, A. 2015, The Astronomer's Telegram, 8374
MacPherson, E., Isler, C. J., Urry, M., et al. 2015, The Astronomer's Telegram, 8382
Malkan, M. A., & Sargent, W. L. W. 1982, ApJ, 254, 22
Marscher, A. P., & Gear, W. K. 1985, ApJ, 298, 114
Marscher, A. P., & Jorstad, S. G. 2011, ApJ, 729, 26
Marscher, A. P., & Scott, J. S. 1980, PASP, 92, 127
Marscher, A. P., Jorstad, S. G., D'Arcangelo, F. D., et al. 2008, Nature, 452, 966
Massaro, E., Giommi, P., Perri, M., et al. 2003, A&A, 399, 33
Medhi, B. J., Maheswar, G., Brijesh, K., et al. 2007, MNRAS, 378, 881
Muneer, S., Stalin, C. S., Venkataramana, A. K., & Baskar, R. 2016, The Astronomer's Telegram, 8806
Neha, S., Maheswar, G., Soam, A., Lee, C. W., & Tej, A. 2016, A&A, 588, A45
Neronov, A., & Vovk, I. 2011, MNRAS, 412, 1389
O'Dell, S. L., Puschell, J. J., Stein, W. A., & Warner, J. W. 1978, ApJS, 38, 267
Paliya, V. S., Muneer, S., Venkataramana, C. S. S. A. K., et al. 2016, The Astronomer's Telegram, 8697
Paliya, V. S., Stalin, C. S., Kumar, B., et al. 2013, MNRAS, 428, 2450
Pursimo, T., Takalo, L. O., Sillanpää, A., et al. 2000, A&AS, 146, 141
Ramaprakash, A. N., Gupta, R., Sen, A. K., & Tandon, S. N. 1998, A&AS, 128, 369
Rautela, B. S., Joshi, G. C., & Pandey, J. C. 2004, Bulletin of the Astronomical Society of India, 32, 159
Romero, G. E., Cellone, S. A., & Combi, J. A. 1999, A&AS, 135, 477
Shakhovskoi, N. M., & Efimov, I. S. 1977, Izvestiya Ordena Trudovogo Krasnogo Znameni Krymskoj Astrofizicheskoj Observatorii, 56, 39
Shappee, B. J., Stanek, K. Z., Holoien, T. W.-S., et al. 2015, The Astronomer's Telegram, 8372
Sillanpaa, A., Haarala, S., Valtonen, M. J., Sundelius, B., & Byrd, G. G. 1988, ApJ, 325, 628
Sillanpaa, A., Takalo, L. O., Kikuchi, S., Kidger, M., & de Diego, J. A. 1991, AJ, 101, 2017
Sillanpaa, A., Takalo, L. O., Nilsson, K., Kidger, M., & de Diego, J. A. 1992, A&A, 254, L33
Sillanpaa, A., Takalo, L. O., Pursimo, T., et al. 1996, A&A, 315, L13
Smith, P. S., Balonek, T. J., Heckert, P. A., & Elston, R. 1986, ApJ, 305, 484
Smith, P. S., Montiel, E., Rightley, S., et al. 2009, ArXiv e-prints, arXiv:0912.3621
Srinivasulu, G., Raveendran, A. V., Muneer, S., et al. 2015, ArXiv e-prints, arXiv:1505.04244
Stalin, C. S., Gopal Krishna, Sagar, R., & Wiita, P. J. 2004, Journal of Astrophysics and Astronomy, 25, 1
Sundelius, B., Wahde, M., Lehto, H. J., & Valtonen, M. J. 1997, ApJ, 484, 180
Takalo, L. O., Sillanpaeae, A., & Nilsson, K. 1994, A&AS, 107
Tommasi, L., Palazzi, E., Pian, E., et al. 2001, A&A, 376, 51
Valtaoja, E., Teräsranta, H., Tornikoski, M., et al. 2000, ApJ, 531, 744
Valtaoja, L., Sillanpaa, A., Valtaoja, E., Shakhovskoi, N. M., & Efimov, I. S. 1991, AJ, 101, 78
Valtonen, M., & Ciprini, S. 2012, Mem. Soc. Astron. Italiana, 83, 219
Valtonen, M., Zola, S., Gopakumar, A., et al. 2015, The Astronomer's Telegram, 8378
Valtonen, M. J., Mikkola, S., Lehto, H. J., et al. 2011, ApJ, 742, 22
Valtonen, M. J., Lehto, H. J., Nilsson, K., et al. 2008, Nature, 452, 851
Valtonen, M. J., Zola, S., Ciprini, S., et al. 2016, ApJL, 819, L37
Villata, M., Raiteri, C. M., Sillanpaa, A., & Takalo, L. O. 1998, MNRAS, 293, L13
Villforth, C., Nilsson, K., Østensen, R., et al. 2009, MNRAS, 397, 1893
Wierzcholska, A., & Siejkowski, H. 2015, The Astronomer's Telegram, 8395
Williamson, K. E., Jorstad, S. G., Marscher, A. P., et al. 2014, ApJ, 789, 135
Xiang, Y., & Dai, B.-Z. 2007, PASJ, 59, 1061
Zhang, L. Z., Fan, J.-H., & Cheng, K.-S. 2002, PASJ, 54, 159
Zola, S., Debski, B., Goyal, A., et al. 2016, The Astronomer's Telegram, 8667

Table 1. Log of photometric observation. Column information are as follows: (1) date of observations; (2) number of data points in DLC; (3) exposure time in second; (4) duration of monitoring in hour. This Table is published in its entirety in the machine-readable format. A portion is shown here for guidance regarding its form and content.

Date	N	Exp. time	Duration
(dd.mm.yyyy)		(s)	(h)
(1)	(2)	(3)	(4)
07.01.2016	2	300	0.2
08.01.2016	3	900	0.9

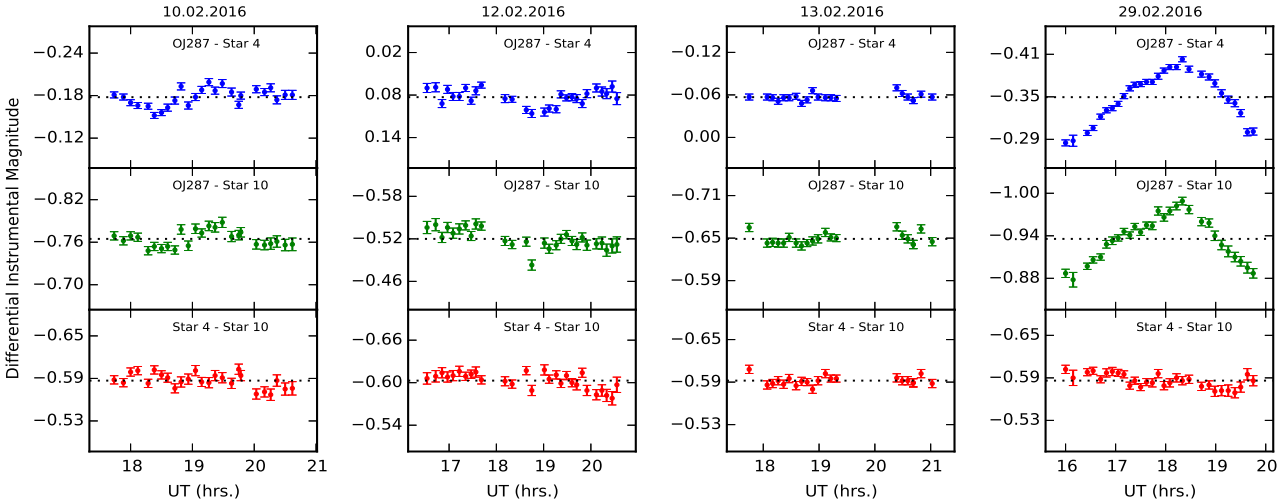

Figure 1. Intra-night DLCs for OJ 287. From top to bottom the DLCs are for OJ 287 - star 4, OJ 287 - star 10 and star 4 - star 10. The dates of observations are written on the top of each panel. The dotted black lines indicate the mean of the DLC. Stars 4 and 10 are those given by Fiorucci & Tosti (1996). Only 4 intra-night DLCs are shown here and the other 17 DLCs are available in the electronic format only.

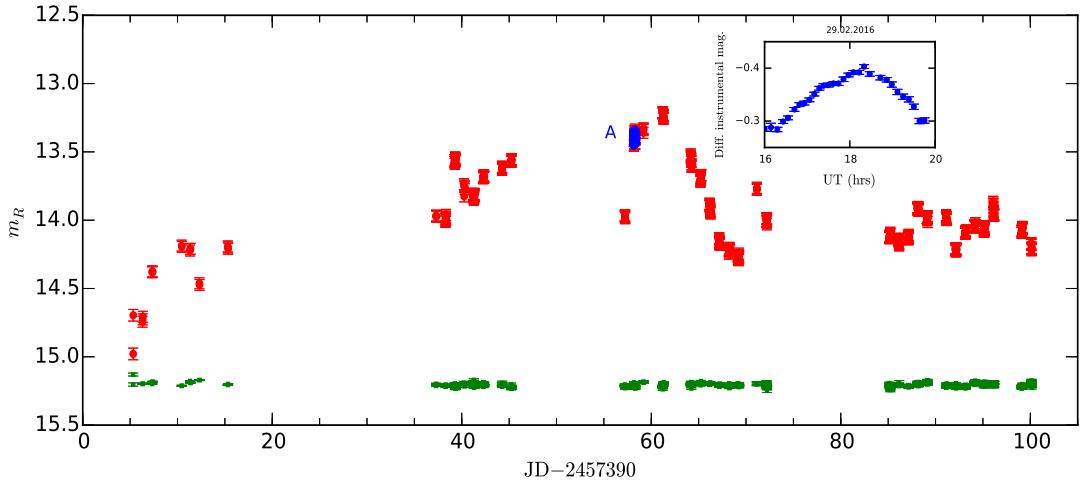

Figure 2. Long term variation of R-band magnitude. The bunch of points in the plots are due to the intra-night monitoring, one such bunch, denoted by "A" includes the DLC of 29 February 2016, shown in the right inset plot. The DLC of star 4 and star 10 is shown at the bottom (square) after shifting by 15.8 mag.

Table 2. Results of polarization observations. Column details are as follows: (1) date of observation; (2) observing band (R' is the integrated polarization in the VRI spectral region); (3) time in Julian Day; (4) degree of polarization in per cent; (5) error in degree of polarization in per cent; (6) polarization position angle in degree; (7) error in position angle in degree.

Date (dd.mm.yyyy) (1)	Band (2)	JD (3)	P (%) (4)	$P_{\rm error}$ (%) (5)	PA (deg.) (6)	$PA_{\rm error}$ (deg.) (7)
12.02.2016	U	2457431.3201	16.3	1.1	110.9	1.9
12.02.2016	B	2457431.3201	18.8	0.8	118.0	1.2
12.02.2016	V	2457431.3648	19.8	1.0	119.0	1.4
12.02.2016	R	2457431.3372	19.2	0.5	115.8	0.8
12.02.2016	I	2457431.3104	16.6	0.3	118.0	1.0
12.02.2016	R'	2457431.2796	18.9	0.3	116.9	0.5
08.03.2016	U	2457456.2399	33.0	1.8	62.4	1.7
08.03.2016	B	2457456.2399	28.6	1.5	59.9	1.6
08.03.2016	R'	2457456.1932	22.6	0.2	60.8	0.3
09.03.2016	R'	2457457.1786	27.7	0.5	61.2	0.5
10.03.2016	U	2457458.2526	38.7	1.4	74.3	1.1
10.03.2016	B	2457458.2526	32.1	1.1	64.9	1.1
10.03.2016	V	2457458.2475	27.8	0.8	71.0	0.9
10.03.2016	R	2457458.2230	28.3	0.8	72.5	0.8
10.03.2016	I	2457458.2870	22.5	0.9	67.3	1.2
10.03.2016	R'	2457458.2012	27.4	0.4	71.6	0.4
11.03.2016	U	2457459.2242	32.2	3.0	63.2	3.1
11.03.2016	B	2457459.2242	27.2	1.6	58.6	1.8
11.03.2016	V	2457459.2232	30.0	0.9	63.5	0.9
11.03.2016	R	2457459.1924	23.7	0.6	60.6	0.8
11.03.2016	R'	2457459.1703	26.7	0.4	61.1	0.5
04.04.2016	U	2457483.1590	24.2	1.9	114.3	2.3
04.04.2016	B	2457483.1590	15.6	1.1	126.5	2.1
04.04.2016	V	2457483.1690	12.7	0.7	123.9	1.7
04.04.2016	R	2457483.1331	15.7	0.7	130.6	1.3
04.04.2016	I	2457483.2047	12.3	0.7	121.5	1.7
04.04.2016	R'	2457483.1112	16.8	0.4	127.5	0.6
05.04.2016	R	2457484.1184	17.0	0.8	107.5	1.4
05.04.2016	R	2457484.1451	15.1	0.8	108.7	1.5
05.04.2016	R	2457484.1666	11.6	0.6	99.1	1.6
05.04.2016	R	2457484.1821	10.1	0.6	115.6	1.8
05.04.2016	R	2457484.1994	12.9	0.7	105.5	1.6
05.04.2016	R	2457484.2221	16.6	0.8	119.9	1.4
06.04.2016	R	2457485.1145	7.6	0.3	112.9	1.3
06.04.2016	R	2457485.1320	6.5	0.4	113.4	1.7
06.04.2016	R	2457485.1491	6.5	0.4	115.5	1.9
06.04.2016	R	2457485.1666	7.3	0.4	116.1	1.5
06.04.2016	R	2457485.1841	6.1	0.5	119.3	2.5
06.04.2016	R	2457485.2012	6.9	0.5	114.4	2.0
06.04.2016	R	2457485.2187	6.2	0.3	113.6	1.6
06.04.2016	R	2457485.2362	6.0	0.3	113.3	1.7
10.04.2016	R	2457489.1125	14.1	0.6	87.7	1.3
10.04.2016	R	2457489.1398	12.5	0.6	89.8	1.4
10.04.2016	R	2457489.1634	12.7	0.6	92.4	1.3
10.04.2016	R	2457489.1869	14.2	0.7	89.9	1.5
10.04.2016	R	2457489.2115	16.2	0.9	90.3	1.6

Table 3. Intra-night variability properties. Column information are: (1) date of observation; (2) and (3) INOV amplitudes in %; (4) and (5) F-values computed for the OJ 287 DLCs relative to the steadiest pair of comparison stars (star 4 and star 10) on any night; (6) variability status according to F-statistics; (7) and (8) values of C for the two OJ 287 DLCs relative to the two comparison stars (star 4 and star 10); (9) variability status as per C-statistics; (10) χ^2 value; (11) critical value $\chi^2_{\alpha=0.01,\nu}$; (12) variability status as per χ^2-statistics; (13) time duration of observation in hour.

Date	$\Psi1$	$\Psi2$	F_1	F_2	Status	C_1	C_2	Status	χ^2	$\chi^2_{\alpha=0.01,\nu}$	Status	dt (hrs.)
(dd.mm.yyyy)	(%)	(%)										
(1)	(2)	(3)	(4)	(5)	(6)	(7)	(8)	(9)	(10)	(11)	(12)	(13)
10.02.2016	4.70	4.00	1.380	1.171	NV	1.175	1.082	NV	163.208	42.980	V	2.2
12.02.2016	4.00	5.80	1.026	1.365	NV	1.013	1.168	NV	122.299	46.963	V	3.1
13.02.2016	2.20	2.70	0.598	1.626	NV	0.773	1.275	NV	26.847	37.566	NV	2.5
29.02.2016	11.80	11.10	12.912	10.753	V	3.593	3.279	V	1932.985	48.278	V	2.9
03.03.2016	4.70	2.10	1.325	0.308	NV	1.151	0.555	NV	281.167	38.932	V	2.2
06.03.2016	9.00	10.30	17.322	14.964	V	4.162	3.868	V	1020.255	37.566	V	2.2
07.03.2016	4.90	5.50	6.707	9.300	V	2.590	3.050	V	284.627	34.805	V	1.8
08.03.2016	7.20	7.20	42.775	43.884	V	6.540	6.625	V	490.736	41.638	V	2.0
09.03.2016	4.80	4.80	9.294	7.986	V	3.049	2.826	V	218.527	37.566	V	1.8
10.03.2016	3.50	4.10	2.440	3.003	NV	1.562	1.733	NV	99.288	34.805	V	2.3
11.03.2016	3.70	3.90	3.916	4.508	V	1.979	2.123	NV	132.167	46.963	V	2.8
27.03.2016	3.89	2.38	1.310	0.471	NV	1.145	0.686	NV	29.150	38.932	NV	2.1
29.03.2016	3.30	3.00	4.958	4.507	V	2.227	2.123	NV	57.634	36.191	V	1.8
30.03.2016	2.70	3.60	0.747	1.174	NV	0.864	1.084	NV	47.865	45.642	V	2.5
31.03.2016	2.00	2.70	1.420	2.111	NV	1.192	1.453	NV	27.399	40.289	NV	2.3
03.04.2016	2.20	2.90	1.476	2.342	NV	1.215	1.530	NV	23.993	38.932	NV	2.0
04.04.2016	2.40	2.40	1.027	1.262	NV	1.013	1.123	NV	24.070	36.191	NV	2.0
05.04.2016	3.00	3.20	0.987	1.305	NV	0.993	1.142	NV	37.446	42.980	NV	2.2
06.04.2016	4.20	5.80	1.200	2.071	NV	1.095	1.439	NV	69.109	42.980	V	2.1
07.04.2016	10.10	10.40	14.908	13.025	V	3.861	3.609	V	484.825	42.980	V	2.2
10.04.2016	4.50	4.70	4.238	6.485	V	2.059	2.547	NV	110.030	40.289	V	2.0

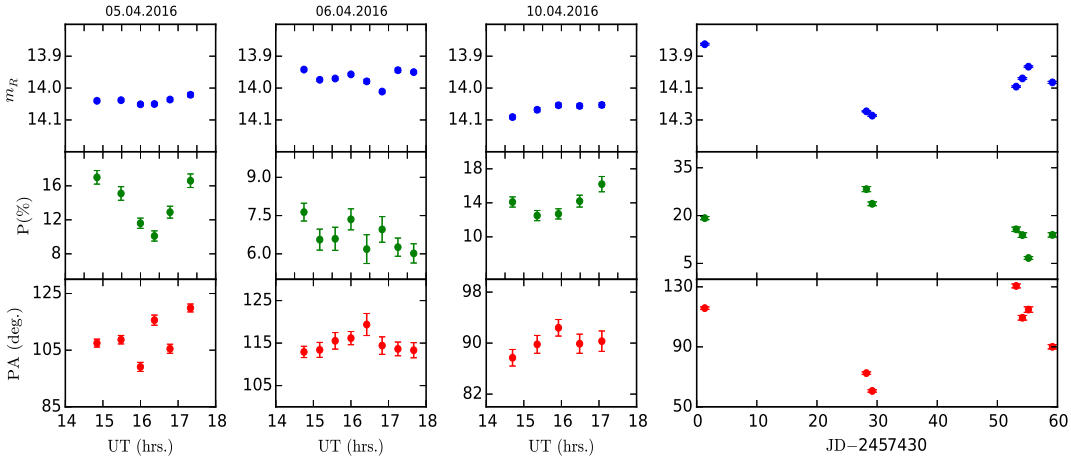

Figure 3. Intra-night polarization variability of OJ 287. Shown from top to bottom are the variation of R-band magnitude (m_R), the degree of polarization (%) and position angle (deg.) as a function of UT (hours.). The dates are shown in the top of each panel. In the right most panel is shown the LTPV of OJ 287.

.

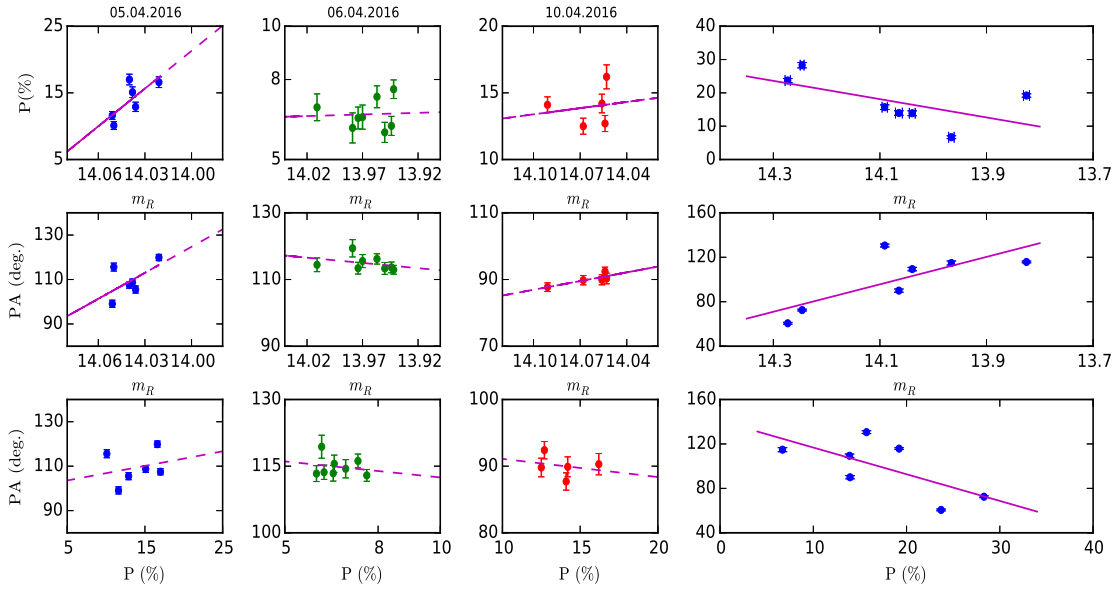

Figure 4. Plots P vs m_R, PA vs m_R and PA vs P for INPV. The dates are indicated on the top of each panel. The right most panel shows the correlation between different physical quantities based on LTPV observations. The lines are the linear least squares fit to the data.

.

Table 4. Results on the correlation analysis between photometric and polarimetric observations. Columns are listed as follows: (1) date of observation; (2) correlation between datasets; (3) Pearson correlation coefficient (r_p); (4) p value for no correlation.

Date	Parameter	r_p	Significance
(1)	(2)	(3)	(4)
All	$F-P$	-0.66	0.000
	$F-PA$	+0.75	0.000
	$P-PA$	-0.62	0.001
05.04.2016	$F-P$	+0.73	0.093
	$F-PA$	+0.57	0.230
	$P-PA$	+0.24	0.635
06.04.2016	$F-P$	+0.04	0.909
	$F-PA$	-0.33	0.416
	$P-PA$	-0.19	0.646
10.04.2016	$F-P$	+0.16	0.787
	$F-PA$	+0.83	0.079
	$P-PA$	-0.24	0.694

Table 5. Intra-night polarization properties. Columns are listed as follows: (1) date of observation; (2) and (3) mean and standard deviation of degree of polarization; (4) Fractional polarization variability; (5) χ^2 of P; (6) Variable (V) /Non-variable (NV); (7) to (11) are the same as (2) to (6) but for position angle.

Date	$< P >$	σ_P	F.V.	χ^2_P	Status	$< PA >$	σ_{PA}	F.V.	χ^2_{PA}	Status
(dd.mm.yyyy)	(%)					($^\circ$)				
(1)	(2)	(3)	(4)	(5)	(6)	(7)	(8)	(9)	(10)	(11)
05.04.2016	13.24	2.552	0.255	80.230	V	109.57	6.759	0.095	117.480	V
06.04.2016	6.73	0.539	0.119	15.701	NV	114.39	2.015	0.028	7.478	NV
10.04.2016	13.62	1.328	0.129	15.380	V	90.01	1.496	0.026	6.598	NV

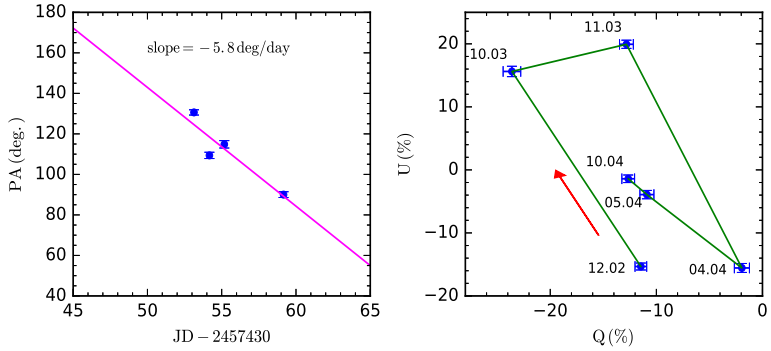

Figure 5. Left: Rotation rate of polarization position angle. A straight line has been fit to the April 2016 polarization data. The estimated slope is −5.8 degree/day. Right: Plot of the equatorial Stokes Q and U parameters in the Q-U plane in *R*-band. The arrow indicates the direction of rotation of the plane of polarization. The labels indicate the date of observations.

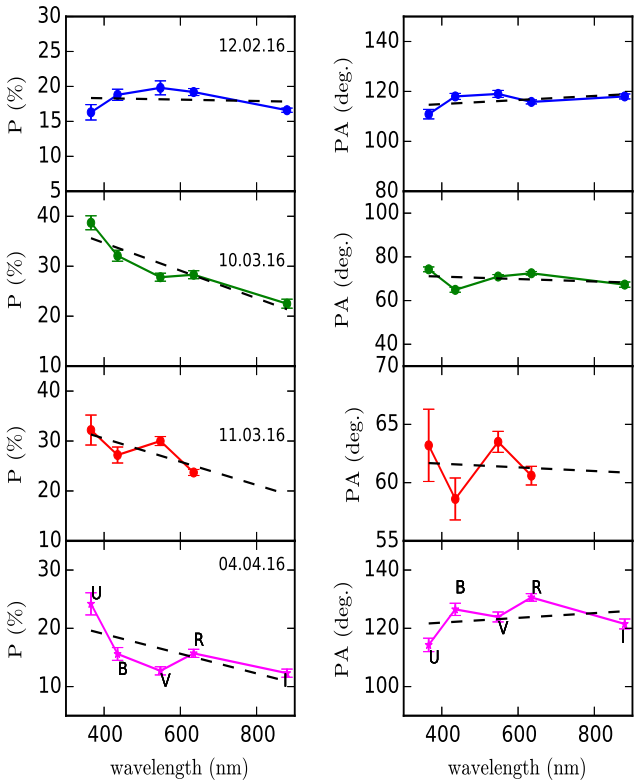

Figure 6. Wavelength dependent polarization. Degree of polarization (left panel) and polarization position angle (right panel) are plotted as a function of wavelength for different dates of observations. The dashed line shows the linear fit to the data. Filter names are marked in the lower panels.

Table 6. Correlation analysis between flux and polarization of OJ 287. Columns are listed as follows: (1) Segment number; (2) Pearson correlation coefficient of P vs V-band magnitude; (3) PA vs V; (4) P vs PA. The p value of no correlation is written within brackets.

Segment	P vs V	PA vs V	PA vs P
(1)	(2)	(3)	(4)
Segment 1	-0.34 (0.45)	-0.56 (0.19)	0.74 (0.0327)
Segment 2	0.55 (0.05)	0.70 (0.01)	0.78 (0.0001)
Segment 3	-0.02 (0.92)	0.10 (0.72)	0.08 (0.7566)

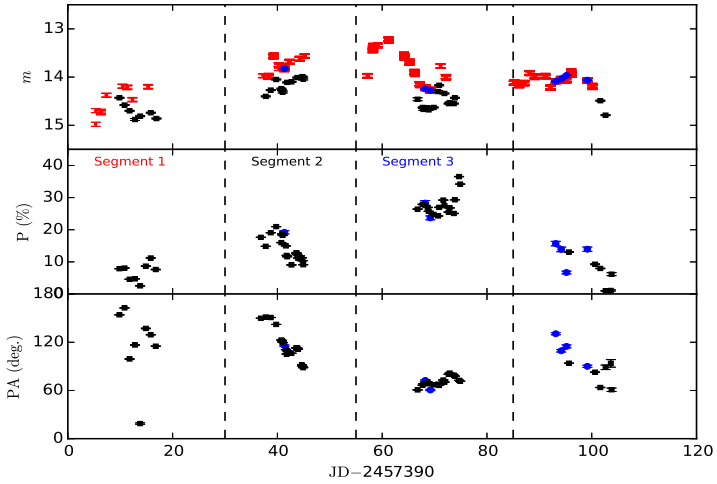

Figure 7. Top: Long term variation of R-band magnitude (m_R) as obtained by us (red) and V-band magnitude (m_V) as obtained by Steward observatory (black). The m_R corresponding to our polarization measurement is shown in blue. Middle: polarization degree from Steward (black) and our (blue). Bottom: Polarization position from Steward (black) and our (blue). The data is divided into different segments for detailed analysis. A clear anticorrelation between brightness and polarization can be seen in Segment 2.

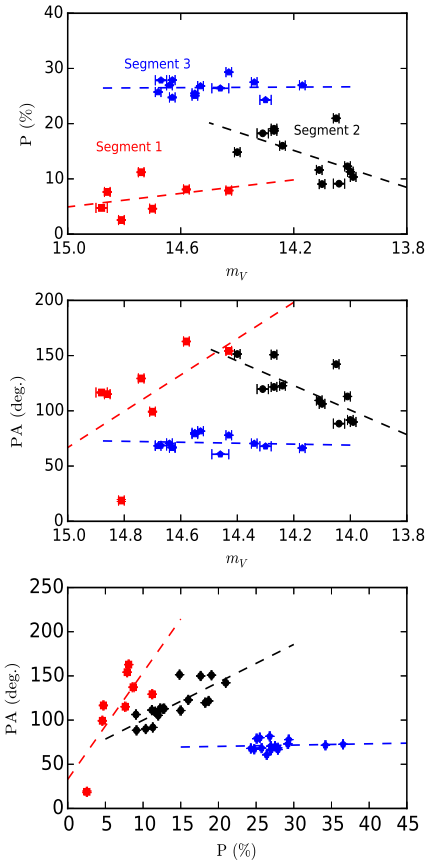

Figure 8. Polarization degree vs V-band magnitude (top), position angle vs V-band magnitude (middle) and position angle vs polarization degree (bottom) for three different segments as presented in Figure 7. The dotted lines represent the linear fit to the data of each segment.